ACS Photonics

Article

pubs.acs.org/journal/apchd5

Hydrogen-Induced Tuning of Plasmon Resonance in Palladium–Silver Layered Nanodimer Arrays

Katsuyoshi Ikeda,*[,†,‡] Sari Uchiyama,[†] Mai Takase,[†,§] and Kei Murakoshi[†]

[†]Division of Chemistry, Graduate School of Science, Hokkaido University, Sapporo 060-0810, Japan

[‡]Japan Science and Technology Agency, PRESTO, 4-1-8 Honcho, Kawaguchi, Saitama 332-0012, Japan

Supporting Information

ABSTRACT: Reversible tuning of localized surface plasmon resonances is achieved with strong resonance intensity in the near-IR region using hydrogen uptake into dimeric nanostructures of Pd–Ag layered nanodots. The resonance feature in the present dimer is characterized by hybridized plasmon modes between two adjacent Pd–Ag layered nanodots with similar plasmonic features. In contrast, the resonance of a conventional Pd–Ag heterodimer is considered to be a perturbed plasmon mode between Pd and Ag nanodots with different plasmonic features. The strong symmetric interactions in the layered dimers lead to a large peak shift with hydrogen uptake into the Pd layers, while the weak asymmetric interactions in the heterodimers result in a decrease in the band intensity. The flexible tailoring of the resonance intensity, wavelength, and tunability of the layered nanostructures provides the possibility for novel functionalized plasmonic materials or devices to be realized.

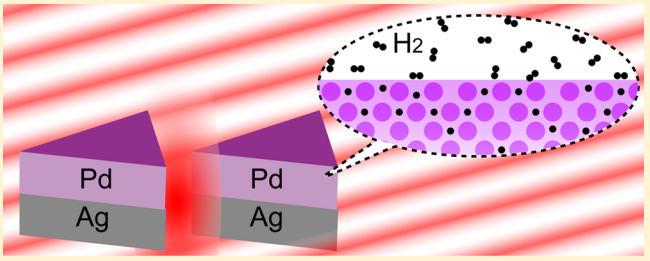

KEYWORDS: *plasmon hybridization, hydrogen uptake, phase transition, multifunctionality*

Nanostructures of noble metals such as gold or silver have recently attracted much interest, due to their characteristic optical properties caused by the resonant excitation of collective oscillations of free electrons on their surface.[1−4] This localized surface plasmon resonance (LSPR) has been widely exploited in various fields such as sensing, spectroscopy, and photochemistry.[5−7] The LSPR feature of a metal nanostructure is characterized by its size and shape, so that a wide wavelength range between the visible and near-infrared regions can be covered by LSPR bands through control of the geometric parameters of these metal nanostructures.[8,9] However, this geometric controllability of the LSPR bands can also be a shortcoming due to difficulty in achieving reversible tuning.[10−13] The achievement of tunable LSPR may open up a novel avenue for plasmonic photochemistry and photonics. To tune the LSPR without changing the geometry of metal nanostructures, it is necessary to control the density or effective mass of free electrons in a metal. The electrochemical shift of the Fermi level in a metal can vary the LSPR wavelength to a very small extent.[14] Another possible method to induce more significant changes is the use of a phase transition such as a metal–insulator transition. To date, one of the most successful attempts to tune the LSPR bands is based on a metal-hydride phase transition.[15−18] Palladium (Pd) can absorb a large amount of hydrogen via formation of palladium hydride (PdH_x), where x is the ratio of H to Pd in the lattice. The density of states at the Fermi level of PdH_x decreases with increasing x, which results in hydrogen-sensitive LSPRs of the Pd nanostructures.[19] This system is expected to be employed for highly sensitive hydrogen sensors, which are an indispensable requirement for hydrogen storage applications. The real-time sensing of hydrogen absorption has thus become a unique tool to understand the kinetic behavior of metal hydride formation.

In spite of the potentiality of such Pd nanostructures, their LSPRs are rather weak in intensity due to their lossy plasmonic nature resulting from the contribution of localized d-electrons at the Fermi level.[20,21] The nature of d-electrons often correlates with physical properties of transition metals such as magnetism or catalytic activity as well as hydrogen absorption. However, strong LSPRs rely on the Drude-like behavior of sp-electrons in noble metal nanostructures, so that the tunability and intensity of the resonance tend to be mutually exclusive. (Recently, it was found that Au nanoparticles were responsive to hydrogen gas only when their LSPR was excited.[22−24] Since this phenomenon is different from the conventional hydrogen uptake-induced LSPR change, we do not discuss it here.) If the tunability and intensity are simultaneously achieved in LSPRs, one can expect to develop active plasmonic devices such as a tunable plasmonic laser, in which hydrogen uptake and release, i.e., tuning of LSPRs, may be electrochemically controlled in the presence of proton sources. Therefore, so-called intensity borrowing from noble metal nanostructures is frequently utilized to obtain stronger LSPRs with transition metal nanostructures.[25−29] For example, when a Pd nanoparticle is

Received: July 3, 2014
Published: December 4, 2014

almost in contact with an Ag or Au nanoparticle, perturbed plasmon modes are built between these two adjacent nanoparticles.[16,17] However, the dominant resonance nature of such bimetal heterodimers is determined by that of the hydrogen-insensitive metal nanoparticle, which results in a rather small hydrogen-induced variation. Recently, Yang et al. reported that Au–Pd trimers with touching Au and Pd nanoparticles showed higher hydrogen sensitivity than Au–Pd dimers, meaning that there is still room for improving the performance of hydrogen response due to geometric optimization in the intensity borrowing system.[18]

In this work, we demonstrate the simultaneous achievement of strong LSPR and large tunability for Pd–Ag layered nanostructure ensembles with ordered arrangements at the centimetric scale. This layered nanostructure array is fabricated using a conventional metal deposition technique combined with the self-assembly of a shadow mask.[30−32] When hydrogen-induced spectral change is rather small, a wide distribution of size and shape in nanostructure ensembles causes a difficulty in observations; indeed, lithographic shape control of nanostructure ensembles or single-nanoparticle observation has usually been conducted in previous investigations.[15−18] Here, a hydrogen-induced effect is clearly observed in the simply fabricated centimetric arrays even under macroscopic observation. The intensity and tunability of the LSPR band can be balanced by changing the thickness ratio of hydrogen-sensitive Pd to plasmonic Ag in the stacked layers of each nanostructure. While conventional Pd–Ag heterodimers are geometrically and optically anisotropic, the present Pd–Ag layered nanodots can be isotropic, which leads to improved flexibility in tailoring functionalized bimetal nanosystems. Dimerization of Pd–Ag layered nanodots can provide much stronger LSPR than that from conventional Pd–Ag heterodimers.

RESULTS AND DISCUSSION

Fabrication of Metal Nanodimer Arrays. Metal nanostructures were fabricated on a glass substrate using angle-resolved nanosphere lithography (AR-NSL).[31,32] The fabrication procedure is illustrated in Figure 1a. One significant advantage of this technique is that the shaped and arrayed nanostructures can be easily formed on a substrate with centimetric size, which enables observation of the optical response using a conventional optical spectrometer. Figure 1b shows a variety of metal nanostructure arrays that were formed using this technique: Ag–Ag dimer, Pd–Pd dimer, Pd–Ag heterodimer, and Pd–Ag layered dimer. Among these structures, the Pd–Pd monometal dimer was utilized to examine the hydrogen uptake effect on the LSPR. For bimetal systems, the conventional heterodimer was used to compare with the present layered dimer with respect to the LSPR intensity and tunability.

Hydrogen Uptake in Pd–Pd Nanodimer Arrays. Figure 2a shows an atomic force microscopy (AFM) image of the Pd–Pd dimer array fabricated with evaporation angles of 0° and 11°. According to our previous study,[31,32] the gap distance is expected to be a few nanometers, although AFM measurement using the conical tip cannot map such morphology. Each dimer consists of two triangular dots with different sizes: a large dot with a length of ca. 120 nm and a small dot with a length of ca. 30 nm. The thickness of the nanodots was approximately 20 nm. These dimers are uniaxially aligned on the substrate, which results in optical anisotropy of the array. Figure 2b shows polarization-dependent extinction spectra of the array, meas-

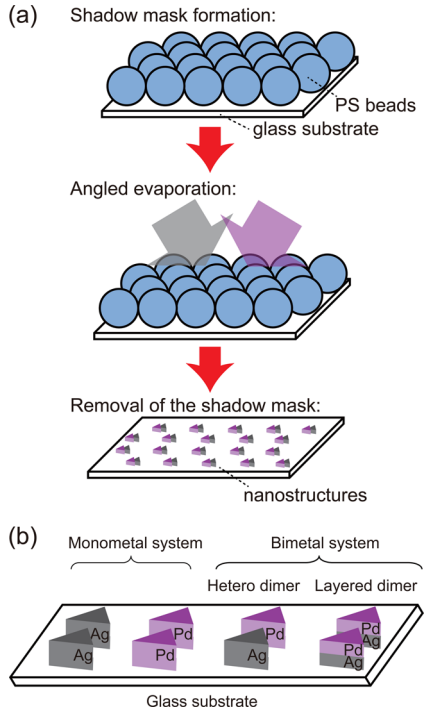

Figure 1. (a) Schematic illustration of the AR-NLS method to fabricate nanodimer arrays on a glass substrate. (b) Variety of dimer systems used in the present study: Ag–Ag and Pd–Pd dimers as monometal systems and Pd–Ag heterodimer and Pd–Ag layered dimers as bimetal systems.

ured using a conventional macroscopic spectrometer (see Methods section for more details). A very broad feature was apparent for each polarization. In particular, the observed band for the long axis was slightly red-shifted compared with that for the short axis. This anisotropic property suggests that these features originate from the LSPR of Pd–Pd dimers.[33,34] The weak and broad resonance is caused by the highly damping nature of the localized d-electrons in Pd. The small peak shift in the long axis polarization implies that the electromagnetic coupling is weak in the dimers. Indeed, the calculated resonance bands are in good agreement with the experimental results, which supports the origin of the spectroscopic features, as shown in Figure 2c. The broader bandwidth in the experimental spectra is probably due to the inhomogeneity of the fabricated nanostructures because the array involves many defects due to the technical limitations of the self-assembled shadow mask in the AR-NSL method.

When this array was exposed to H_2–Ar mixed gas with a H_2 partial pressure of 3×10^3 Pa under atmospheric pressure at room temperature, spectral variations were observed for both polarization directions. Figure 3a shows the difference spectra for the array with and without H_2, which indicates that the LSPR of the Pd nanostructures is indeed affected by hydrogen uptake. From a comparison of Figures 2b and 3a, it was concluded that hydrogen uptake into the Pd nanostructures induces a decrease in the LSPR intensity. Figure 3b shows a time course of the spectral variation at 600 nm measured for the long-axis polarization. When H_2 gas was introduced to the cell, the LSPR intensity quickly decreased and then reached equilibrium. After the H_2–Ar gas flow was interrupted by alternating N_2 gas flow, the resonance intensity gradually recovered to the initial value. This hydrogen-induced change

dx.doi.org/10.1021/ph500242c | ACS Photonics 2015, 2, 66−72

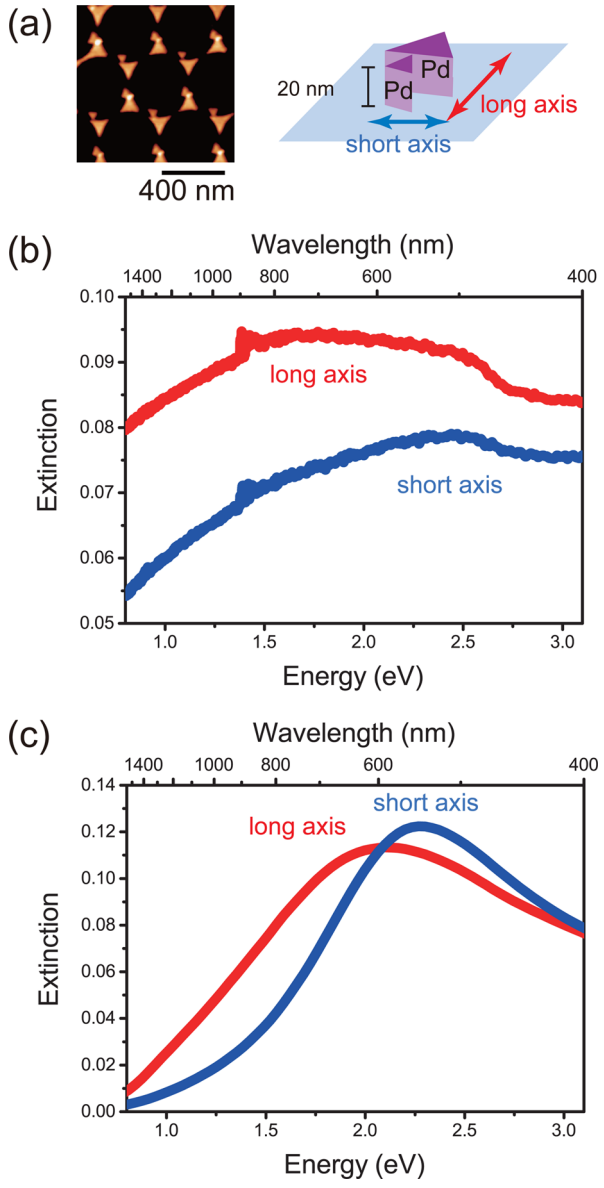

Figure 2. (a) AFM image and details of the Pd−Pd dimer array. (b) Extinction spectra for the Pd−Pd dimer array measured along the long and short axes of the ordered dimers. (c) Theoretically calculated extinction spectra for the Pd−Pd dimer array.

was repeated several times, but the recovery rate gradually decreased as shown in Figure S1.

When Pd absorbs hydrogen, two different phases of PdH_x, i.e., a solid solution (α phase) and hydride (β phase), are formed depending on the atomic ratio of $x = H/Pd$, where $x \leq 1$. (Figure S2 shows approximate pressure−composition isotherms for the Pd-PdH phase in bulk Pd exposed to a hydrogen atmosphere.[35]) It is assumed that the optical constants of the β phase are significantly different from those of metallic Pd.[36] From previous reports, there is a consensus that the hydrogen-induced variation of LSPR correlates with the β phase formation in Pd nanostructures.[15,37] Figure 4 shows the decrease in LSPR intensity at 600 nm, measured parallel to the long axis of Pd−Pd dimers, as a function of both temperature and the H_2 partial pressure under atmospheric pressure. The induced variations are larger at lower temperature under higher H_2 pressure; significant changes were observed in

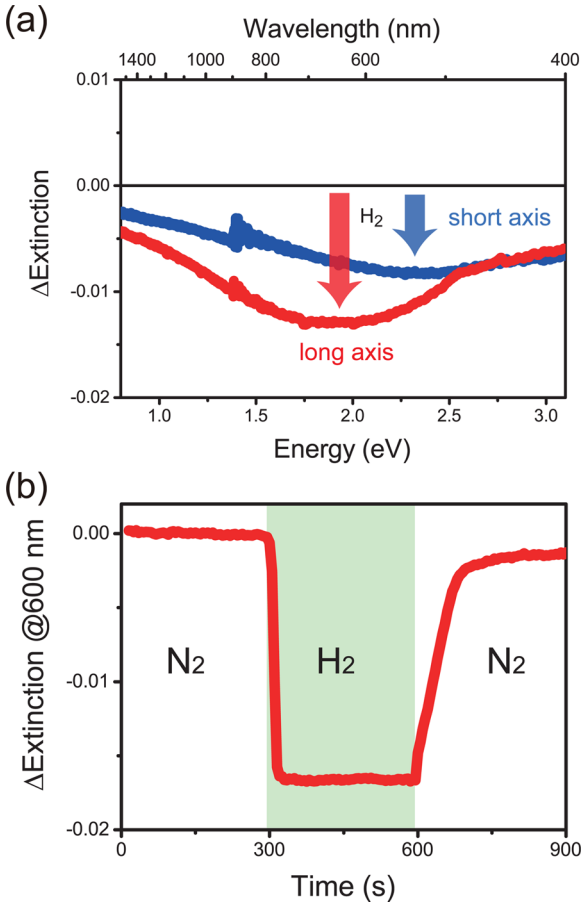

Figure 3. (a) Difference spectra for the Pd−Pd dimer array with and without H_2 gas with a partial pressure of 3×10^3 Pa under atmospheric pressure at room temperature. (b) Temporal behavior of the long-axis LSPR intensity at 600 nm with and without H_2 gas under the same conditions as (a).

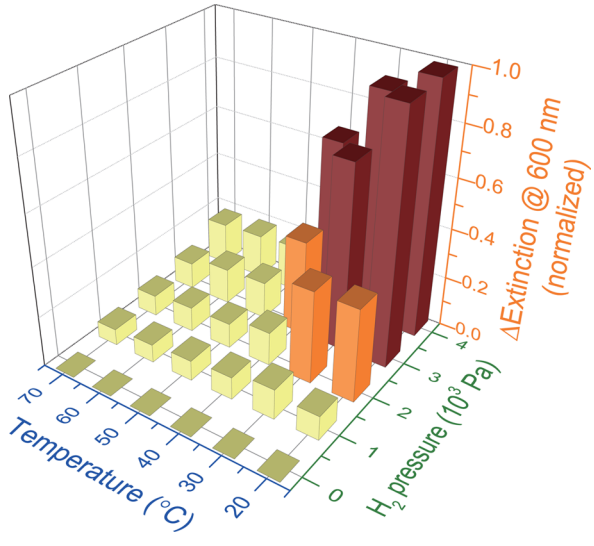

Figure 4. Hydrogen-induced variations of the long-axis LSPR intensity of Pd−Pd dimers at 600 nm as a function of temperature and H_2 partial pressure under atmospheric pressure. A series of LSPR changes measured for various partial pressures at each temperature were normalized with respect to the magnitude of the change induced by pure H_2 gas.

dx.doi.org/10.1021/ph500242c | ACS Photonics 2015, 2, 66−72

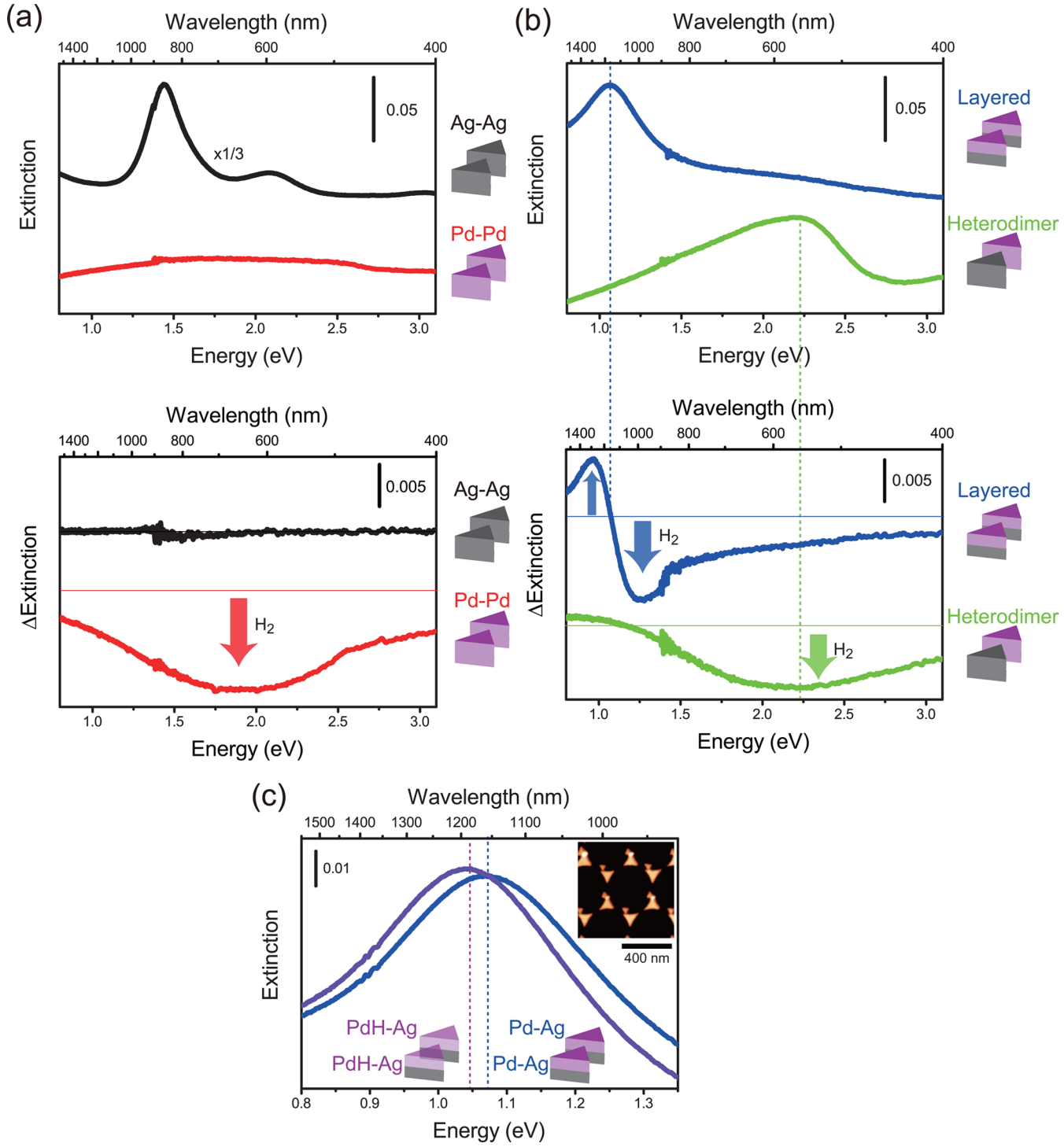

Figure 5. (a) Extinction spectra and hydrogen-induced variations for the monometal Ag−Ag and Pd−Pd dimers. (b) Extinction spectra and hydrogen-induced variations for the bimetal Pd−Ag heterodimer and Pd−Ag layered dimers. (c) Enlarged spectra for the Pd−Ag layered dimers with and without H_2 gas. The inset shows an AFM image of the Pd−Ag layered dimers.

the low-temperature region between 20 and 40 °C when the H_2 pressure was higher than 2×10^3 Pa. In the high-temperature region above 50 °C, no such variation was observed under the present pressure conditions. The pressure dependence of the LSPR variations conforms well to the phase diagram shown in Figure S2. That is, at room temperature and under atmospheric pressure, the LSPR characteristics of the Pd nanostructure array vary sensitively in the presence of a few percent H_2 gas through the formation of the β-phase PdH_x with $x > 0.6$. In the meantime, the phase transition to β-phase results in a lattice expansion as much as 4%. In the dimer system, thus, the formation of the β-phase may cause a decrease of the gap distance.[18] However, we could not elucidate this contribution to the observed LSPR change because there were many structural defects in the array due to the fabrication method; the pressure and temperature dependences measured along the short axis were similar to those along the long axis.

dx.doi.org/10.1021/ph500242c | ACS Photonics 2015, 2, 66−72

Hydrogen Uptake in Pd−Ag Nanodimer Arrays. To increase the LSPR intensity, Pd nanostructures may be combined with Ag or Au nanostructures.[16−18] This concept is conventionally realized as a Pd−Ag heterodimer, as shown in Figure 1b. However, the LSPR of this structure is predominantly determined by that of the Ag nanostructure, resulting in a decrease of tunability. Alternatively, a Pd−Ag layered nanodot can be considered to achieve intensity and tunability simultaneously because the optical properties of this structure roughly resemble that of a mixture of Pd and Ag, according to the effective medium approach (see Supporting Information for a detailed discussion).[38] The layered nanodots can be dimerized, as shown in Figure 1b, so that the LSPR property would be flexibly tailored, although phase retardation is non-negligible in a strongly interacting dimer.[33] In all of the dimers examined here, i.e., Ag−Ag and Pd−Pd dimers, and Pd−Ag heterodimer and layered dimers, the thickness of the nanodots was fixed at 20 nm. For the layered system, 10 nm Ag layers were formed on the substrate followed by deposition of 10 nm Pd layers. Hydrogen-induced spectral variations were obtained at room temperature and atmospheric pressure with a H_2 partial pressure of 3×10^3 Pa.

Figure 5a shows extinction spectra for the Ag−Ag and Pd−Pd monometal dimers and their difference spectra with and without H_2 measured with the polarization direction parallel to the dimer axis. As already explained in Figures 2 and 3, the LSPR band of the Pd−Pd dimers was extremely weak and broad due to the lossy electronic nature of Pd, while the LSPR intensity was reversibly changed upon exposure to the hydrogen atmosphere. In contrast, the Ag−Ag dimer showed a very intense LSPR band at 850 nm but no significant hydrogen-induced effect.

Figure 5b shows extinction spectra for the Pd−Ag heterodimer and Pd−Ag layered dimer arrays and their difference spectra with and without H_2. Both bimetal structures exhibit a clear LSPR band, which is much larger than that for the Pd−Pd dimer array. Moreover, the peak position is completely different between these two bimetal systems. The Pd−Ag heterodimer has a broad LSPR band at around 550 nm with a low-energy tail. It is noted that this peak position is very close to that of the Ag monomer. The low-energy tail is probably due to the contribution of the Pd nanodot. In contrast, the Pd−Ag layered dimer exhibits a sharp LSPR band at 1200 nm. The largely red-shifted band suggests that the electromagnetic coupling between nanodots is strong in the layered dimer. That is, a wide-wavelength region can be covered by the LSPR of this system, in a similar manner to that for conventional monometal dimers. This flexible tailoring of the resonance wavelength is a significant advantage in the layered system.

In addition to the difference in the static resonance feature, the hydrogen-induced response was significantly different between these two bimetal systems. In the case of the heterodimers, the hydrogen-induced variation appeared as a decrease in the LSPR band intensity; the spectral variation was the largest at the peak wavelength of the LSPR band. However, in the layered dimers, the spectral variation exhibited a differential feature with a minimum at the peak wavelength of the LSPR band. The enlarged raw spectra of Figure 5c show that this corresponds to a peak shift of ca. 30 nm. The layered system is thus much better than the heterodimer system with respect to the simultaneous achievement of resonance intensity and tunability. Moreover, the LSPR intensity and tunability can be balanced by changing the thickness ratio of Pd to Ag (see Figure S4).

CONCLUSION

In the geometry-specific LSPR features of metal nanostructures, simultaneous achievement of LSPR intensity and tunability was realized using the dimer structures of Pd−Ag layered nanodots. In this structure, creation of strongly interacting hybridized plasmon modes enables the flexible tailoring of the LSPR intensity, wavelength, and tunability. The formation of layered structures does not affect hydrogen uptake into the Pd layers of stacked nanodots; therefore, the optical properties and hydrogen responsivity can be individually considered in the layered system. Moreover, the layered system is much better for use in the near-IR region. Actually, these advantages are not limited to hydrogen-sensitive Pd, but are applicable to various transition metals. For example, layered nanostructures of plasmonic Au and magnetic Ni or Co may realize large magneto-plasmonic responses.[40] Achievement of multifunctional plasmonic materials with strong resonances in the near-IR region could lead to novel applications or devices in the fields of sensing, spectroscopy, and photochemistry.

METHODS

The fabrication procedure of metal nanostructure arrays using AR-NSL is illustrated in Figure 1a.[31,32] First, a hexagonally packed monolayer of 350 nm diameter polystyrene (PS) beads was self-assembled on a glass substrate as a shadow mask for vacuum evaporation. Double-angle evaporation of Ag or Pd was then conducted through the shadow mask. The PS bead monolayer was then removed to obtain regularly aligned metal nanostructures on the substrate. The aspect ratio of each nanostructure was adjusted by varying the evaporation angle and the thickness of the evaporated metal films.

Optical transmission measurements of the nanostructure arrays were performed from the top of the samples through a gas-flow cell with transparent windows. The flow cell was filled with N_2 gas or H_2−Ar mixed gas with a specific H_2 partial pressure under atmospheric pressure, which was continuously provided from a gas cylinder. The temperature of the substrate was controlled on a transparent thermoplate (MATS-1002RN, Tokai Hit Co., Ltd.), which was utilized as one of the cell windows. Equilibrium broadband spectra and transient spectral variations for the arrays were measured using a UV/vis/NIR spectrometer (V-670, Jasco) and a spectro multichannel photodetector (MPD-311C, Otsuka Electronics), respectively.

Theoretical calculations of extinction spectra were conducted using the finite-difference time-domain (FDTD) method (FDTD Solutions, Lumerical Solutions, Inc.). In the calculation, the extinction cross sections for each nanostructure unit were calculated and extinction spectra were then obtained with the assumption that electromagnetic interactions between nanostructure units were negligible. The dielectric functions of Ag and Pd were obtained from the literature.[39]

ASSOCIATED CONTENT

Supporting Information

We show cyclic responses of LSPR in a Pd nanosystem for hydrogen exposure, pressure−composition isotherms for the Pd−PdH phase, LSPR bands of Ag−Pd layered monomers, and thickness dependence of LSPR in Pd−Ag layered dimers. This

dx.doi.org/10.1021/ph500242c | ACS Photonics 2015, 2, 66−72

material is available free of charge via the Internet at http://pubs.acs.org.

AUTHOR INFORMATION

Corresponding Author

*E-mail: kikeda@pchem.sci.hokudai.ac.jp.

Present Address

[§]Catalysis Research Center, Hokkaido University, Sapporo 001-0021, Japan.

Notes

The authors declare no competing financial interest.

ACKNOWLEDGMENTS

This research was supported in part by Grants-in-Aid for Young Scientists (A) (No. 24681018) and for Exploratory Research (No. 24651126) from the Japan Society for the Promotion of Science (JSPS), World Premier International Research Center (WPI) Initiative on Materials Nanoarchitechtonics, and the Program for Development of Environmental Technology using Nanotechnology from the Ministry of Education, Culture, Sports, Science and Technology (MEXT), Japan. The authors also acknowledge Dr. Vyacheslav Silkin for kind provision of the dielectric functions for PdH_x systems.

REFERENCES

(1) Barnes, W. L.; Dereux, A.; Ebbesen, T. W. Surface Plasmon Subwavelength Optics. *Nature* **2003**, *424*, 824−830.

(2) Bharadwaj, P.; Deutsch, B.; Novotny, L. Optical Antennas. *Adv. Opt. Photonics* **2009**, *1*, 438−483.

(3) Halas, N. J.; Lal, S.; Chang, W. S.; Link, S.; Nordlander, P. Plasmons in Strongly Coupled Metallic Nanostructures. *Chem. Rev.* **2011**, *111*, 3913−3961.

(4) Morton, S. M.; Silverstein, D. W.; Jensen, L. Theoretical Studies of Plasmonics Using Electronic Structure Methods. *Chem. Rev.* **2011**, *111*, 3962−3994.

(5) Kneipp, K.; Kneipp, H.; Itzkan, I.; Dasari, R. R.; Feld, M. S. Ultrasensitive Chemical Analysis by Raman Spectroscopy. *Chem. Rev.* **1999**, *99*, 2957−2975.

(6) Hartschuh, A. Tip-Enhanced Near-Field Optical Microscopy. *Angew. Chem., Int. Ed.* **2008**, *47*, 8178−8191.

(7) Choi, H.; Chen, W. T.; Kamat, P. V. Know Thy Nano Neighbor. Plasmonic versus Electron Charging Effects of Metal Nanoparticles in Dye-Sensitized Solar Cells. *ACS Nano* **2012**, *5*, 4418−4427.

(8) Zeman, E. J.; Schatz, G. G. An Accurate Electromagnetic Theory Study of Surface Enhancement Factors for Ag, Au, Cu, Li, Na, Al, Ga, In, Zn, and Cd. *J. Phys. Chem.* **1987**, *91*, 634−643.

(9) Sun, Y.; Xia, Y. Gold and Silver Nanoparticles: A Class of Chromophores with Colors Tunable in the Range from 400 to 750 nm. *Analyst* **2003**, *128*, 686−691.

(10) Sershen, S. R.; Westcott, S. L.; Halas, N. J.; West, J. L. Independent Optically Addressable Nanoparticle-Polymer Optomechanical Composites. *Appl. Phys. Lett.* **2002**, *80*, 4609−4611.

(11) Olcum, S.; Kocabas, A.; Ertas, G.; Atalar, A.; Aydinli, A. Tunable Surface Plasmon Resonance on an Elastometric Substrate. *Opt. Express* **2009**, *17*, 8542−8547.

(12) Ahonen, P.; Schiffrin, D. J.; Paprotny, J.; Kontturi, K. Optical Switching of Coupled Plasmons of Ag-Nanoparticles by Photoisomerization of an Azobenzene Ligand. *Phys. Chem. Chem. Phys.* **2007**, *9*, 651−658.

(13) Jin, R.; Cao, Y. W.; Mirkin, C. A.; Kelly, K. L.; Schatz, G. C.; Zheng, J. G. Photoinduced Conversion of Silver Nanospheres to Nanoprisms. *Science* **2001**, *294*, 1901−1903.

(14) Templeton, A. C.; Pietron, J. J.; Murray, R. W.; Mulvaney, P. Solvent Refractive Index and Core Charge Influences on the Surface Plasmon Absorbance of Alkanethiolate Monolayer-Protected Gold Clusters. *J. Phys. Chem. B* **2000**, *104*, 564−570.

(15) Langhammer, C.; Zoric, I.; Kasemo, B.; Clemens, B. M. Hydrogen Storage in Pd Nanodisk Characterized with a Novel Nanoplasmonic Sensing Scheme. *Nano Lett.* **2007**, *7*, 3122−3127.

(16) Liu, N.; Tang, M. L.; Hentschel, M.; Giessen, H.; Alivisatos, A. P. Nanoantenna-Enhanced Gas Sensing in a Single Tailored Nanofocus. *Nat. Mater.* **2011**, *10*, 631−636.

(17) Shegai, T.; Johansson, P.; Langhammer, C.; Käll, M. Directional Scattering and Hydrogen Sensing by Bimetallic Pd-Au Nanoantennas. *Nano Lett.* **2012**, *12*, 2464−2469.

(18) Yang, A.; Huntington, M. D.; Cardinal, M. F.; Masango, S. S.; Van Duyne, R. P.; Odom, T. W. Hetero-Oligomer Nanoparticle Arrays for Plasmon-Enhanced Hydrogen Sensing. *ACS Nano* **2014**, *8*, 7639−7647.

(19) Silkin, V. M.; Chernov, I. P.; Echenique, P. M.; Koroteev, Y. M.; Chulkov, E. V. Influence of Hydrogen Absorption on Low-Energy Electronic Collective Excitations in Palladium. *Phys. Rev. B* **2007**, *76*, 245105.

(20) Langhammer, C.; Kasemo, B.; Zoric, I. Absorption and Scattering of Light by Pt, Pd, Ag, and Au Nanodisks: Absolute Cross Sections and Branching Ratios. *J. Chem. Phys.* **2007**, *126*, 194702.

(21) Tian, Z. Q.; Yang, Z. L.; Ren, B.; Wu, D. Y. SERS from Transition Metals and Excited by Ultraviolet Light. *Top, Appl. Phys.* **2006**, *103*, 125−146.

(22) Mukherjee, S.; Libisch, F.; Large, N.; Neumann, O.; Brown, L. V.; Cheng, J.; Lassiter, J. B.; Carter, E. A.; Nordlander, P.; Halas, N. J. Hot Electrons Do the Impossible: Plasmon-Induced Dissociation of H_2 on Au. *Nano Lett.* **2013**, *13*, 240−247.

(23) Mukherjee, S.; Zhou, L.; Goodman, A. M.; Large, N.; Ayala-Orozco, C.; Zhang, Y.; Nordlander, P.; Halas, N. J. Hot-Electron-Induced Dissociation of H_2 on Gold Nanoparticles Supported on SiO_2. *J. Am. Chem. Soc.* **2014**, *136*, 64−67.

(24) Sil, D.; Gilroy, K. D.; Niaux, A.; Boulesbaa, A.; Neretina, S.; Borguet, E. Seeing Is Believing: Hot Electron Based Gold Nanoplasmonic Optical Hydrogen Sensor. *ACS Nano* **2014**, *8*, 7755−7762.

(25) Mrozek, M. F.; Xie, Y.; Weaver, M. J. Surface-Enhanced Raman Scattering on Uniform Platium-Group Overlayers: Preparation by Redox Replacement of Underpotential-Deposited Metals on Gold. *Anal. Chem.* **2001**, *73*, 5953−5960.

(26) Hu, J.; Tanabe, M.; Sato, J.; Uosaki, K.; Ikeda, K. Effects of Atomic Geometry and Electronic Structure of Platinum Surfaces on Molecular Adsorbates Studied by Gap-Mode SERS. *J. Am. Chem. Soc.* **2014**, *136*, 10299−10307.

(27) Li, J. F.; Huang, Y. F.; Ding, Y.; Yang, Z. L.; Li, S. B.; Zhou, Z. S.; Fan, F. R.; Zhang, W.; Zhou, Z. Y.; Wu, D. Y.; Ren, B.; Wang, Z. L.; Tian, Z. Q. Shell-Isolated Nanoparticle-Enhanced Raman Spectroscopy. *Nature* **2010**, *464*, 392−395.

(28) Ikeda, K.; Sato, J.; Uosaki, K. Surface-Enhanced Raman Scattering at Well-Defined Single Crystalline Faces of Platinum-Group Metals Induced by Gap-Mode Plasmon Excitation. *J. Photochem. Photobiol. A* **2011**, *221*, 175−180.

(29) Ikeda, K.; Sato, J.; Fujimoto, N.; Hayazawa, N.; Kawata, S.; Uosaki, K. Plasmonic Enhancement of Raman Scattering on Non-SERS-Active Platinum Substrates. *J. Phys. Chem. C* **2009**, *113*, 11816−11821.

(30) Hulteen, J. C.; Treichel, D. A.; Smith, M. T.; Duval, M. L.; Jensen, T. R.; Van Duyne, R. P. Nanosphere Lithography: Size-Tunable Silver Nanoparticle and Surface Cluster Arrays. *J. Phys. Chem. B* **1999**, *103*, 3854−3863.

(31) Ikeda, K.; Takase, M.; Sawai, Y.; Nabika, H.; Murakoshi, K.; Uosaki, K. Hyper-Raman Scattering Enhanced by Anisotropic Dimer-Plasmons on Artificial Nanostructures. *J. Chem. Phys.* **2007**, *127*, 111103.

(32) Ikeda, K.; Takase, M.; Hayazawa, N.; Kawata, S.; Murakoshi, K.; Uosaki, K. Plasmonically Nano-Confined Light Probing Invisible Phonon Modes in Defect-Free Graphene. *J. Am. Chem. Soc.* **2013**, *135*, 11489−11492.

(33) Nordlander, P.; Oubre, C.; Prodan, E.; Li, K.; Stockman, M. I. Plasmon Hybridization in Nanoparticle Dimers. *Nano Lett.* **2004**, *4*, 899−903.
(34) Sheikholeslami, S.; Jun, Y. W.; Jain, P. K.; Alivisatos, A. P. Coupling of Optical Resonances in a Compositionally Asymmetric Plasmonic Nanoparticle Dimer. *Nano Lett.* **2010**, *10*, 2655−2660.
(35) Manchester, F. D.; San-Martin, A.; Pitre, J. M. The H-Pd (Hydrogen-Palladium) System. *J. Phase Equilib.* **1994**, *15*, 62−83.
(36) Silkin, V. M.; Díez Muiño, R.; Chernov, I. P.; Chulkov, E. V.; Echenique, P. M. Tuning the Plasmon Energy of Palladium-Hydrogen Systems by Varying the Hydrogen Concentration. *J. Phys.: Condens. Matter* **2012**, *24*, 104021.
(37) Poyli, M. A.; Silkin, V. M.; Chernov, I. P.; Echenique, P. M.; Díez Muiño, R.; Aizpurua, J. Multiscale Theoretical Modeling of Plasmonic Sensing of Hydrogen Uptake in Palladium Nanodisks. *J. Phys. Chem. Lett.* **2012**, *3*, 2556−2561.
(38) Aspnes, D. E. Plasmonics and Effective-Medium Theories. *Thin Solid Films* **2011**, *519*, 2571−2574.
(39) Lynch, D. W.; Hunter, W. R. Comments on the Optical Constants of Metals and an Introduction to the Data for Several Metals. In *Handbook of Optical Constants of Solids*; Palik, E. D., Ed.; Academic Press: Verlag, 1997; pp275−367.
(40) Bonanni, V.; Bonetti, S.; Pakizeh, T.; Pirzadeh, Z.; Chen, J.; Nogués, J.; Vavassori, P.; Hillenbrand, R.; Akerman, J.; Dmitriev, A. Designer Magnetoplasmonics with Nickel Nanoferromagnets. *Nano Lett.* **2011**, *11*, 5333−5338.